

Observation of a sequential process in charge-asymmetric dissociation of CO_2^{q+} ($q = 4,5$) upon the impact of highly charged ions

Arnab Khan, Lokesh C. Tribedi, and Deepankar Misra*

Department of Nuclear and Atomic Physics, Tata Institute of Fundamental Research, Homi Bhabha Road, Colaba, Mumbai 400005, India

(Received 4 June 2015; published 8 September 2015)

The dynamics involved in three-body breakup of carbon dioxide upon the impact of 1-MeV Ar^{8+} ions is investigated. Among the six possible fragmentation channels of CO_2^{q+} ($q = 4,5$), where all fragments are charged, two charge-asymmetric fragmentation channels show evidence of a sequential breakup process. It has been observed that the molecular structures tend towards deformed geometry as the initial charge on the precursor molecular ion increases. The total energy deposition to the system is found to play a key role in deciding between different breakup pathways.

DOI: [10.1103/PhysRevA.92.030701](https://doi.org/10.1103/PhysRevA.92.030701)

PACS number(s): 34.50.Gb

The basic understanding of the decay dynamics of polyatomic molecules is a topic of current and fundamental interest [1,2]. In recent time, much importance has been given to answer the question whether the three-body fragmentation happens via concerted or sequential processes for molecules such as CO_2 , CS_2 , carbonyl sulfide, or even bigger molecules such as 1,3-butadiene [1–4]. Very recently, sequential and concerted pathways in fragmentation of CS_2 have been identified as the two possible outcomes (opening and not opening the box) of the famous “Schrödinger’s cat” paradox [2]. However, it still remains as a big challenge, both experimentally and theoretically, to understand the complex dynamics involved in the ion-induced breakup of these molecules. When a highly charged ion interacts with a molecule one or many electrons can be removed from the molecule by various processes, namely, ionization, electron capture, capture ionization, etc. After the ionization, the remaining electrons get redistributed inside the molecule within a time scale of attoseconds to femtoseconds [5]. Following this, the nuclei also rearrange themselves to find a possible equilibrium on the potential energy surface; this may eventually lead to the breaking of bonds. In the case of diatomic molecules it is seen that symmetric charge sharing is more probable than asymmetric charge sharing [6]. On the contrary, for rare-gas dimers an asymmetric channel has been found to be the preferred one [7]. For polyatomic molecules the situation can be much more complicated owing to the coupling between various electronic and nuclear degrees of freedom.

In the past, several studies have been carried out on the fragmentation of CO_2 as a prototype system upon the impacts of heavy ions [1,8–11], photons [12–15], and electrons [16–20]. Earlier heavy ion impact studies on CO_2 were either performed at very high velocities [8,9] where the ionization process dominates over other processes, or at very low velocity collisions [1,11] where capture is the most dominant channel. However, the detailed study of fragmentation dynamics of CO_2^{q+} in the intermediate velocity regime is scarce. In the present study, we have chosen intermediate velocity (1 a.u.) Ar^{8+} ions, where both capture and ionization processes are equally probable. Most of the earlier works mainly

concentrated on the decay dynamics of CO_2^{3+} or were only limited to the kinetic energy release (KER) distribution studies. The concept of a sequential breakup process in three-body breakup of triatomic molecules has been a topic of discussion for quite some time now [21,22]. However, it is only recently that Neumann *et al.* [1], demonstrated the existence of sequential as well as concerted fragmentation processes in charge exchange collisions of highly charged ions with CO_2 . Following this, Wu *et al.* [13] and Wang *et al.* [20] have also showed the presence of concerted and sequential breakup channels for femtosecond laser-induced ionization and electron impact ionization of CO_2 , respectively. Recently, Wu *et al.* [23] performed experiments to study the breakup dynamics of CO_2^{q+} ($q = 3–6$) in some of the symmetric channels and did not find any evidence of a sequential breakup pathway for CO_2^{q+} ($q = 4–6$). In this Rapid Communication we show the existence of both concerted as well as sequential breakup channels in *charge-asymmetric* fragmentation of CO_2^{q+} ($q = 4,5$).

The present experiment has been carried out at the Electron Cyclotron Resonance based ion accelerator at the Tata Institute of Fundamental Research in Mumbai [24,25]. The three-dimensional momentum vectors are derived from the measured time of flight and the position of the detected fragment ions using the recoil ion momentum spectroscopy technique. The details of the experimental setup are described elsewhere [26]. Briefly, a beam of Ar^{8+} ions is intersected with an effusive jet of CO_2 gas. After the interaction, daughter ions are extracted perpendicular to the projectile beam direction and projected onto a multihit capable time and position sensitive detector system. An extraction field of 173.3 V cm^{-1} followed by an accelerating field of 250.6 V cm^{-1} is used in the experiment. The signal from a channel electron multiplier is used as a trigger to the data acquisition system.

After the molecule gets multiply charged, Coulomb force leads to the breakup of the molecular ion. This can happen through various pathways such as concerted and sequential processes. In the concerted process both the $\text{C} = \text{O}$ bonds break simultaneously and the oxygen ions take away almost equal amounts of kinetic energy. In the sequential process, first, one of the two $\text{C} = \text{O}$ bonds breaks and the second $\text{C} = \text{O}$ bond breaks after a delay. Figures 1(a)–1(c) show the Dalitz plots [27] for the three-body breakup of CO_2^{q+} ($q = 3–5$). The

*dmsira@tifr.res.in

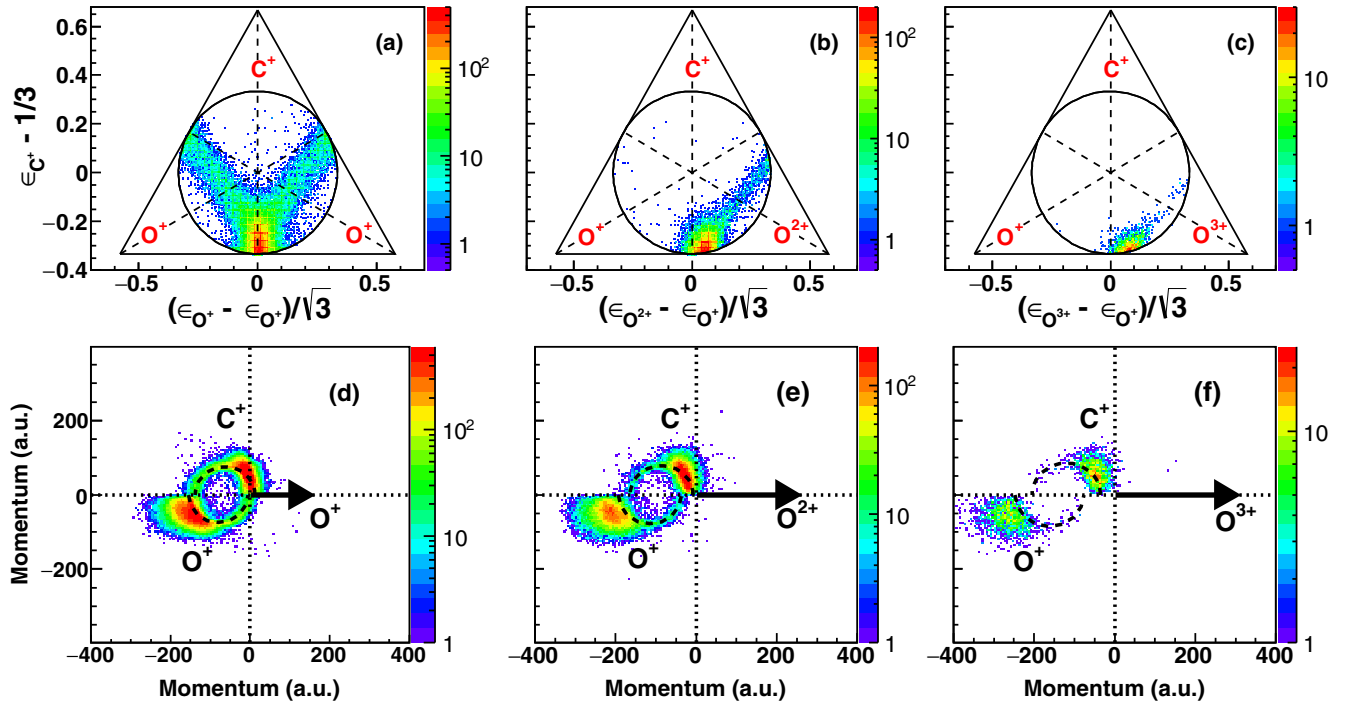


FIG. 1. (Color online) (a)–(c) Dalitz plots for three-body fragmentation CO_2^{q+} ($q = 3\text{--}5$). (d)–(f) Newton diagrams for CO_2^{q+} ($q = 3\text{--}5$) fragmentation. Black dashed semicircles show the sequential process.

Dalitz plot is a very useful representation to visualize three-body breakup dynamics in which the coordinates are defined as $X\text{-Dalitz} = (\epsilon_1 - \epsilon_2)/\sqrt{3}$ and $Y\text{-Dalitz} = \epsilon_3 - 1/3$ with $\epsilon_i = |P_i|^2 / \sum_i |P_i|^2$, where P_i is the momentum of the detected ion in the center-of-mass frame and $i \in \{O^{1+/2+/3+}, O^+, C^+\}$. This plot represents the partitioning of momentum to all the fragment ions for three-body dissociation processes in phase space. Conservation of energy requires all points to lie within a triangle of unit height, whereas conservation of momentum demands all points to lie within a circle of radius $1/3$. In Fig. 1(a) we observe an intense region around $X\text{-Dalitz} = 0$ and $Y\text{-Dalitz} = -1/3$, which corresponds to the concerted decay process. Considering the linear geometry of the CO_2 molecule it is also expected that in the case of the concerted process the momentum is shared mainly between the two O^+ ions leaving the C^+ ion with very low momentum. It is seen from Fig. 1(a), that the distribution extends from $Y\text{-Dalitz} = -1/3$ to -0.1 representing the bent geometry of CO_2^{3+} ions. The winglike structures on the right and left sides of the $X\text{-Dalitz} = 0$ line are the signature of the sequential fragmentation process where one O^+ is removed from CO_2^{3+} leaving a metastable CO^{2+} ion which successively dissociates into C^+ and O^+ ions. During the first bond breakup, the CO^{2+} intermediate acquires some angular momentum and, consequently, can rotate while dissociating [1,13]. If the lifetime of the CO^{2+} ion is more than (or at least of same order) the half-rotational time period of the CO^{2+} ion, then semicircular structures will be seen in the Newton diagrams [1,2]. In Figs. 1(d) and 1(e), we plot the experimental Newton diagrams for CO_2^{q+} ions fragmenting into the constituent atomic ions. Here, e.g., in Fig. 1(d) we have shown the direction of the first O^+ ions, in the center-of-mass frame, along the x axis (represented by a black arrow and

the length of the arrow corresponds to the peak value of the momentum distribution). Momentum components of C^+ and O^+ , parallel and perpendicular to this vector, are plotted in the upper and the lower half, respectively. In the Newton plot we observe two semicircular structures along with two bright crescentlike structures [cf. Fig. 1(d)]. The semicircular and the crescentlike structures correspond to sequential and concerted processes, respectively.

Now the question is whether a sequential process would be observed for CO_2^{q+} ($q > 3$) or not. In fragmentation of CO_2^{4+} we observe $O^{2+} + C^+ + O^+$ [in short (2,1,1)] and (1,2,1) channels with branching ratios of 0.62 : 0.38. Whereas, for CO_2^{5+} fragmentation, (2,2,1), (2,1,2), (3,1,1), and (1,3,1) channels have branching ratios given by 0.518 : 0.379 : 0.084 : 0.017. In order to study a sequential mechanism, first we have chosen two different asymmetric channels of CO_2^{4+} and CO_2^{5+} , namely, (2,1,1) and (3,1,1), particularly because in both these channels there is a possibility of a metastable intermediate CO^{2+} . If we imagine the fragmentation of CO_2^{4+} is happening purely via sequential processes, there could be two channels, $\text{CO}_2^{4+} \rightarrow O^{2+} + \text{CO}^{2+}$ and $\text{CO}_2^{4+} \rightarrow O^+ + \text{CO}^{3+}$. Similarly, for CO_2^{5+} possible channels are $\text{CO}_2^{5+} \rightarrow O^{3+} + \text{CO}^{2+}$ and $\text{CO}_2^{5+} \rightarrow O^+ + \text{CO}^{4+}$. As if for sequential fragmentation, both the channels are entangled. Figures 1(b) and 1(c) show the Dalitz plots for these two channels. We see prominent distributions around $(\epsilon_{O^{2+}/O^{3+}} - \epsilon_{O^+})/\sqrt{3} = 0.05/0.08$, which indicate that most of the fragmentation proceeds via a concerted process with a slightly deformed structure of the parent ions. We also notice a weak linear trace of density distributions on the right side of both the plots which correspond to the sequential fragmentation channel. In Figs. 1(b) and 1(c) we see only

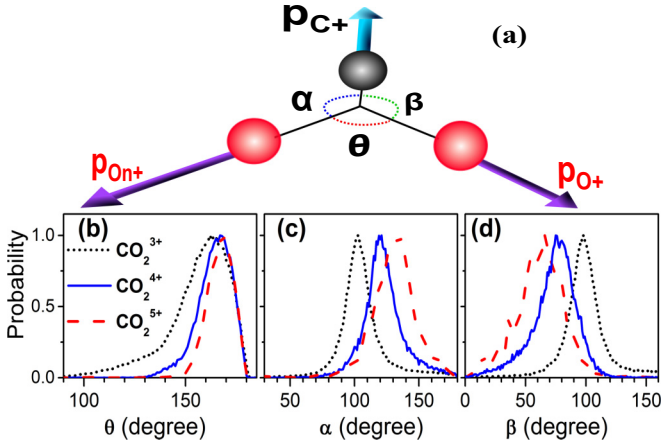


FIG. 2. (Color online) (a) A schematic diagram of three-body fragmentation of CO_2^{q+} [$q = 3-5$ and $n = (q - 2)$], where all the momenta and angles are defined in the center-of-mass frame. (b)–(d) Probability distribution are defined in the center-of-mass frame as defined in (a).

one wing in the Dalitz plots as opposed to the two wings in Fig. 1(a). From this we can directly conclude that the sequential fragmentation of CO_2^{4+} and CO_2^{5+} occurs only via $\text{O}^{2+} + \text{CO}^{2+}$ and $\text{O}^{3+} + \text{CO}^{2+}$ channels. We also observe semicircular structures in the Newton plots [cf. Figs. 1(e) and 1(f)] indicating rotation of CO^{2+} . In the case of the (1,1,1) channel 20.3% of the total events come from the sequential decay, which gives quantitatively very good agreement with the previous experimental result [1]. However, for the (2,1,1) and (3,1,1) channels the contributions are 8.8% and 4.5%, respectively. No trace of a sequential mechanism has been observed for the other decay channels mentioned above.

To further understand the molecular geometry just before the fragmentation process, we have plotted the angles between the correlated momentum vectors of fragment ions in the center-of-mass frame (cf. Fig. 2). Figure 2(b) shows that the peak value of angle θ changes from 163° to 170° as the charge state of the parent ion increases. Similarly the peak values of α increase from 97° to 135° and the peak values of β decrease from 102° to 66° [cf. Figs. 2(c) and 2(d)] with increasing charge states. This can be understood from a pure Coulombic picture: as the charge difference between two O ions increases the Coulomb force also increases and, as a result, θ shifts towards the higher charge side with sharper distributions. As C^+ experiences a more repulsive force from the $\text{O}^{3+}/\text{O}^{2+}$ side than from the O^+ side α increases and β decreases accordingly. In Newton diagrams we also see [cf. Figs. 1(d) and 1(e)] the centroid of the distributions of C^+ ions shifts from 0 a.u. to -50 a.u. as the charge state increases from 3 to 5, resulting from the extra momentum gain due to the bent geometry of the molecular ions.

In order to understand the energetics of the fragmentation mechanism in a detailed manner, we have plotted the Dalitz plots for the breakup of CO_2^{q+} ions corresponding to different KER regions (cf. Fig. 3). In the KER region between 10 and 19 eV, for CO_2^{3+} , the sequential process is most dominant and the concerted process takes over the sequential process as KER increases. For the fragmentation of CO_2^{4+} and CO_2^{5+}

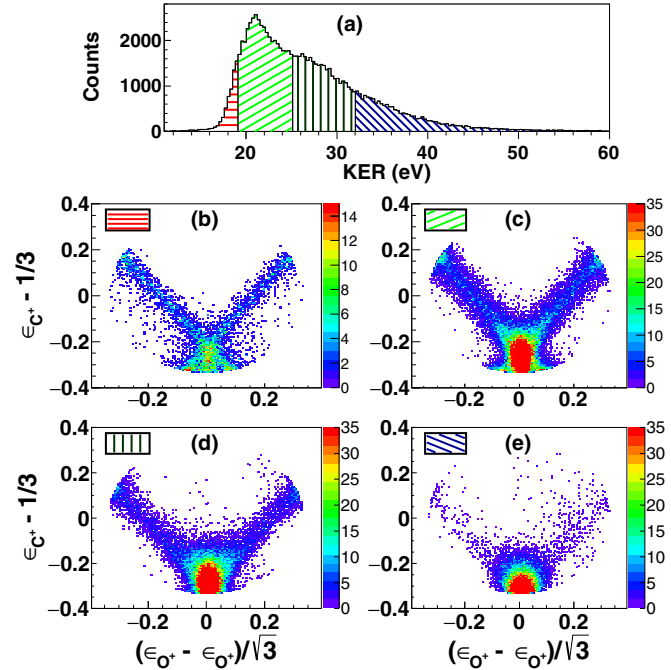


FIG. 3. (Color online) (a) KER spectrum for the fragmentation of CO_2^{3+} . Dalitz plots for different KER regions: (b) 10–19 eV, (c) 19–25 eV, (d) 25–32 eV, and (e) 32–60 eV.

we observe a similar behavior (cf. Fig. 4). In these two cases, the lower part of the KER distributions (20–45 eV for CO_2^{4+} and 55–74 eV for CO_2^{5+}) are mostly contributed from the sequential process and with the increase of KER values the concerted process becomes dominant (cf. Fig. 4). In all three channels, we can see contributions of the sequential

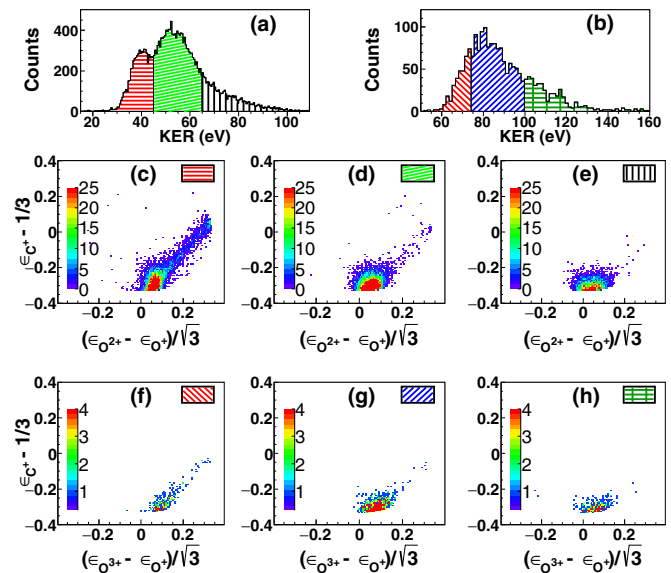


FIG. 4. (Color online) (a) KER spectrum for the fragmentation of CO_2^{4+} , (2,1,1). (b) KER spectrum for the fragmentation of CO_2^{5+} , (3,1,1). Dalitz plots for different KER regions of CO_2^{4+} : (c) 20–45 eV, (d) 45–65 eV, and (e) 65–100 eV. Dalitz plots for different KER regions of CO_2^{5+} : (f) 55–74 eV, (g) 74–100 eV, and (h) 100–160 eV.

process becoming almost negligible for higher KER values. A similar behavior has been observed before for CO_2^{3+} in collision with slow highly charged ions [1]. From this analysis we can conclude that the low-lying states of molecular ions are populated when energy deposition is small and the sequential fragmentation is preferred. With the increase of energy deposition higher electronic states get excited and increase the probability of concerted decay.

A close inspection of different Newton diagrams in Fig. 1 indicates the following: In each case, two center shifted semicircular distributions are observed which correspond to the rotation of the long-lived CO^{2+} intermediate. For CO_2^{3+} fragmentation, the values of the radius, the centers of C^+ and O^+ distributions are around 75, -63 , and -80 a.u., respectively. The same quantities for CO_2^{4+} are found to be 78, -86 , and -115 a.u. For CO_2^{5+} these quantities are 85, -123 , and -165 a.u. It can also be noted that this shift, in the centers of the semicircular distributions, tends to increase with the initial charge state of the precursor molecular ion. A simple kinematical calculation shows that the centers of the momentum distributions of C^+ (P_{C^+}), O^+ (P_{O^+}), and the shift in the centers, δp , depend on the center-of-mass momentum, $P_{\text{CO}^{2+}}$, the masses of C (m_{C^+}), and O (m_{O^+}) obeying the following relations:

$$P_{\text{C}^+} = \left(\frac{m_{\text{C}^+}}{m_{\text{O}^+} + m_{\text{C}^+}} \right) P_{\text{CO}^{2+}}, \quad (1)$$

$$P_{\text{O}^+} = \left(\frac{m_{\text{O}^+}}{m_{\text{O}^+} + m_{\text{C}^+}} \right) P_{\text{CO}^{2+}}, \quad (2)$$

$$\delta p = \left| \frac{m_{\text{O}^+} - m_{\text{C}^+}}{m_{\text{O}^+} + m_{\text{C}^+}} \right| P_{\text{CO}^{2+}}. \quad (3)$$

From the momentum distributions in Figs. 1(d)–1(f), we find the values of δp to be 17, 29, and 42 a.u., respectively. These correspond to the center-of-mass momenta of 119, 203, and 294 a.u. for the CO^{2+} moiety. This implies that most of the KER in sequential fragmentation comes from the motion of the center-of-mass of the CO^{2+} moiety and the first O^+ ion (about 10, 30, and 63 eV for charge states 3, 4, and 5, respectively) leaving only a small amount of internal excitation energy in the CO^{2+} which eventually dissociates. This probably explains the existence of the counterintuitive sequential process where such high excitation energies are involved in the breakup of CO_2^{4+} and CO_2^{5+} . From the most probable values of the radii of semicircles for the three cases we calculate the KER values of 6.0, 6.5, and 7.8 eV for the fragmentation of CO^{2+} moiety as the second step of sequential decay.

Figure 5 shows KER spectra (calculated in the center-of-mass frame of CO^{2+}) of $\text{CO}^{2+} \rightarrow \text{C}^+ + \text{O}^+$ fragmentation. These spectra are generated by putting conditions on the

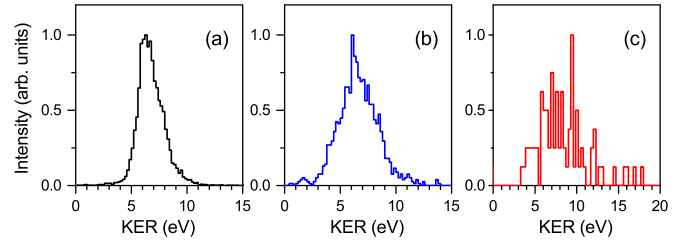


FIG. 5. (Color online) KER spectra of the $\text{CO}_2^{2+} \rightarrow \text{C}^+ + \text{O}^+$ channel calculated in the center-of-mass frame of CO_2^{2+} for sequential fragmentation: (a) CO_2^{3+} , (b) CO_2^{4+} , and (c) CO_2^{5+} .

sequential decay parts (wings in the Dalitz plots) in all three cases. It is seen that the mean KER values are very close to the KER values derived using radii of the semicircles in the Newton diagrams. Here it would be interesting to compare our observation with the K -shell photoelectron angular distributions reported by Weber *et al.* [cf. Figs. 4(a)–4(f) of Ref. [28]]. Figure 4(a) of Ref. [28] shows the photoelectron angular distribution for KER range 6.0–7.0 eV which is quite different than the expected one. However, in Figs. 4(b)–4(d) of Ref. [28] the expected angular distributions are attenuated, but still visible to some extent (KER range 7.0–10.0 eV). On the contrary, for the KER values more than 10.2 eV [Figs. 4(e) and 4(f) of Ref. [28]] the photoelectron angular distributions perfectly match with the expected ones. This loss of angular memory in the photoelectron spectrum for KER below 10.2 eV, especially within 6.0–7.0 eV, was attributed to the rotation of CO^{2+} prior to the fragmentation. In this respect our result matches quite well with the result of Weber *et al.* [28]. From these KER values we can probably conclude that $^1\Pi$ and $^3\Sigma^+$ states are getting populated during the fragmentation of CO_2^{3+} and CO_2^{4+} [29], while in case of CO_2^{5+} the contributing states can be $^1\Pi$, $^3\Sigma^+$, and $2^1\Sigma^+$ [29].

In conclusion, our measurements provide a new level of insight into the molecular fragmentation of CO_2 . We have shown that both concerted and sequential fragmentation channels are present in the fragmentation of CO_2^{q+} which is not seen in previous studies for charge states higher than $3+$. We have also studied molecular geometries of CO_2^{q+} and observed a systematic change in the geometrical structure which tends towards a deformed geometry as the charge state of the parent ion increases. Along with these, this study also shows that the energy deposition to the system plays a key role to decide whether a sequential or a concerted channel will be dominant during fragmentation. It is observed that, irrespective of the charge state of the parent molecular ion, the internal energy of the CO^{2+} fragment is always around the same value.

We wish to acknowledge K. V. Thulasiram and W. A. Fernandes for their help during ECR operation.

[1] N. Neumann, D. Hant, L. P. H. Schmidt, J. Titze, T. Jahnke, A. Czasch, M. S. Schöffler, K. Kreidi, O. Jagutzki, H. Schmidt-Böcking, and R. Dörner, *Phys. Rev. Lett.* **104**, 103201 (2010).

[2] R. Guillemin, P. Declava, M. Stener, C. Bomme, T. Marin, L. Journel, T. Marchenko, R. K. Kushawaha, K. Jänkälä, N. Trcera, K. P. Bowen, D. W. Lindle, M. N. Piancastelli, and M. Simon, *Nat. Commun.* **6**, 6166 (2015).

- [3] B. Wales, T. Motojima, J. Matsumoto, Z. Long, W.-K. Liu, H. Shiromaru, and J. Sanderson, *J. Phys. B* **45**, 045205 (2012).
- [4] L. Zhang, S. Roither, X. Xie, D. Kartashov, M. Schöffler, H. Xu, A. Iwasaki, S. Gräfe, T. Okino, K. Yamanouchi, A. Baltuska, and M. Kitzler, *J. Phys. B* **45**, 085603 (2012).
- [5] F. Remacle and R. D. Levine, *Proc. Natl. Acad. Sci. USA* **103**, 6793 (2006).
- [6] I. Ben-Itzhak, S. G. Ginther, and K. D. Carnes, *Phys. Rev. A* **47**, 2827 (1993).
- [7] J. Matsumoto, A. Leredde, X. Flechard, K. Hayakawa, H. Shiromaru, J. Rangama, C. L. Zhou, S. Guillous, D. Hennecart, T. Muranaka, A. Mery, B. Gervais, and A. Cassimi, *Phys. Rev. Lett.* **105**, 263202 (2010).
- [8] M. R. Jana, P. N. Ghosh, B. Bapat, R. K. Kushawaha, K. Saha, I. A. Prajapati, and C. P. Safvan, *Phys. Rev. A* **84**, 062715 (2011).
- [9] L. Adoui, T. Muranaka, M. Tarisien, S. Legendre, G. Laurent, A. Cassimi, J.-Y. Chesnel, X. Fléhard, F. Frémont, B. Gervais, E. Giglio, and D. Hennecart, *Nucl. Instrum. Methods Phys. Res., Sect. B* **245**, 94 (2006).
- [10] L. Adoui, M. Tarisien, J. Rangama, P. Sobocinsky, A. Cassimi, J.-Y. Chesnel, F. Frémont, B. Gervais, A. Dubois, M. Krishnamurthy, S. Kumar, and D. Mathur, *Phys. Scr. T* **92**, 89 (2001).
- [11] J. H. Sanderson, T. Nishide, H. Shiromaru, Y. Achiba, and N. Kobayashi, *Phys. Rev. A* **59**, 4817 (1999).
- [12] Z. D. Pešić, D. Rolles, R. C. Bilodeau, I. Dimitriu, and N. Berrah, *Phys. Rev. A* **78**, 051401 (2008).
- [13] C. Wu, C. Wu, D. Song, H. Su, Y. Yang, Z. Wu, X. Liu, H. Liu, M. Li, Y. Deng, Y. Liu, L.-Y. Peng, H. Jiang, and Q. Gong, *Phys. Rev. Lett.* **110**, 103601 (2013).
- [14] C. Wu, G. Zhang, C. Wu, Y. Yang, X. Liu, Y. Deng, H. Liu, Y. Liu, and Q. Gong, *Phys. Rev. A* **85**, 063407 (2012).
- [15] I. Bocharova, R. Karimi, E. F. Penka, J.-P. Brichta, P. Lassonde, X. Fu, J.-C. Kieffer, A. D. Bandrauk, I. Litvinyuk, J. Sanderson, and F. Légaré, *Phys. Rev. Lett.* **107**, 063201 (2011).
- [16] C. Tian and C. R. Vidal, *Phys. Rev. A* **58**, 3783 (1998).
- [17] X. Wang, Y. Zhang, D. Lu, G. C. Lu, B. Wei, B. H. Zhang, Y. J. Tang, R. Hutton, and Y. Zou, *Phys. Rev. A* **90**, 062705 (2014).
- [18] P. Bhatt, R. Singh, N. Yadav, and R. Shanker, *Phys. Rev. A* **85**, 042707 (2012).
- [19] B. Bapat and V. Sharma, *J. Phys. B* **40**, 13 (2007).
- [20] E. Wang, X. Shan, Z. Shen, M. Gong, Y. Tang, Y. Pan, K.-C. Lau, and X. Chen, *Phys. Rev. A* **91**, 052711 (2015).
- [21] E. Krishnakumar, V. Krishnamurthi, F. A. Rajgara, U. T. Raheja, and D. Mathur, *Phys. Rev. A* **44**, R4098 (1991).
- [22] S. Hsieh and J. H. D. Eland, *J. Phys. B* **30**, 4515 (1997).
- [23] C. Wu, C. Wu, Y. Fan, X. Xie, P. Wang, Y. Deng, Y. Liu, and Q. Gong, *J. Chem. Phys.* **142**, 124303 (2015).
- [24] A. N. Agnihotri, A. H. Kelkar, S. Kasthurirangan, K. V. Thulasiram, C. A. Desai, W. A. Fernandez, and L. C. Tribedi, *Phys. Scr. T* **144**, 014038 (2011).
- [25] S. Kasthurirangan, A. N. Agnihotri, C. A. Desai, and L. C. Tribedi, *Rev. Sci. Instrum.* **83**, 073111 (2012).
- [26] A. Khan, L. C. Tribedi, and D. Misra, *Rev. Sci. Instrum.* **86**, 043105 (2015).
- [27] R. Dalitz, *London Edinburgh Dubl. Philos. Mag. J. Sci.* **44**, 1068 (1953).
- [28] T. Weber, O. Jagutzki, M. Hattass, A. Staudte, A. Nauert, L. Schmidt, M. H. Prior, A. L. Landers, A. Bräuning-Demian, H. Bräuning, C. L. Cocke, T. Osipov, I. Ali, R. D. Muiño, D. Rolles, F. J. G. de Abajo, C. S. Fadley, M. A. V. Hove, A. Cassimi, H. Schmidt-Böcking, and R. Dörner, *J. Phys. B* **34**, 3669 (2001).
- [29] M. Lundqvist, P. Baltzer, D. Edvardsson, L. Karlsson, and B. Wannberg, *Phys. Rev. Lett.* **75**, 1058 (1995).